Integrate-and-Reset Feedback and Feedforward for a Solenoid With Unknown Parameters

Riccardo Bertollo, Michael Schwegel, Andreas Kugi, Luca Zaccarian

Integrate-and-reset feedback and feedforward for a solenoid with unknown parameters

Riccardo Bertollo, , Michael Schwegel, , Andreas Kugi, , Luca Zaccarian,

***Abstract*— We propose a hybrid feedback-feedforward control scheme for output current tracking in a solenoid, based on an integrate-and-reset paradigm. The feedback, based on a First-Order Reset Element, produces stabilizing inputs comprising diverging exponentials, inducing an aggressive feedback correction. The feedforward uses a hybrid recursive least-squares method with directional forgetting. The hybrid nature of the control loop allows using non-exponentially stable filters, which preserve the past information, as opposed to the stable filters typically used in the adaptive control literature. We prove stability of both the estimation and the tracking error, also using a novel result on forward invariance of a desirable set where the information matrix evolves. Experimental results confirm the effectiveness of the proposed hybrid control scheme.**

I. Introduction

Controlling solenoid-based actuators is challenging due to large variations of unknown parameters, mostly caused by manufacturing tolerances, changing environmental conditions or degradation. Classical strategies include PID control, internal model control (IMC) and sliding mode control (SMC) [10], [17], featuring high robustness, often at the expense of tracking performance [16]. Recent advances in nonlinear hybrid dynamical systems [8], which combine continuous and discrete evolution of their states, allowed to revisit the historical "reset control" strategy of [4] and provide Lyapunov-based tools for stability analysis. These tools enable a suggestive "integrate and reset" paradigm, allowing for aggressive exponentially diverging branches of feedback actions with dead-beat reset actions, stemming from a suitable feedforward signal [1], [11], [15]. Integrate-and-reset control of electromechanical systems was shown in [6], [13], with a rudimentary adaptive feedforward, further developed in [5], where the feedforward adaptations are performed using converging input-output filters.

In this paper, we improve upon the work in [5] by following the "integrate and reset" paradigm also for these feedforward-related filters. Specifically, we employ non-converging filters, such as integrators, which have the advantage of guaranteeing that none of the gathered information is lost before the adaptation time. At suitable jump times, all of the information is used, then the filters are reset to zero, ensuring the boundedness of their output. In this setting, we manage to prove convergence properties of an adaptation law stemming from the well-known recursive least squares (RLS) estimation method. Recent works [9], [12] show that RLS possesses desirable boundedness properties, further improved by directional forgetting [3], [14] to ensure boundedness of the information matrix, for which we prove here a new explicit bound. As compared to [2], we address here three additional challenges. First, we prove the preassigned explicit lower and upper bounds for the information matrix, which were only introduced as a conjecture in [2]. Second, while only simulation results were given in [2], we include here experimental validation of the proposed control scheme by multiple tests on a commercial solenoid. Last, we propose an event-triggered adaptation mechanism, which replaces the typical periodic logic and could be exploited to ensure properties like persistence of excitation, thus improving the robustness of the adaptive scheme against parameter drift.

The paper is organized as follows. In Sections II and III we describe the feedback and feedforward components, respectively. In Section IV we report the closed-loop stability analysis. Experiments are finally reported in Section V.

Notation: Denote $(x_1,\ x_2) := \left[x_1^\top, x_2^\top\right]^\top$. Following [8], for a hybrid solution $\phi(t,j)$, parametrized by continuous time t and discrete time j, $\dot{\phi}$ characterizes its derivative with respect to t and ϕ^+ its next value with respect to j.

II. Hybrid Feedback Stabilization

A good approximation of a solenoid dynamics from the voltage input u to the current output y (see [16, §2]) is

$$\dot{y} = a_p y + b_p u + \bar{d}, \tag{1}$$

where $\bar{d}$ is a constant unknown bias, and $a_p = -R_L/L, b_p = 1/L$ (where L is the solenoid inductance and R_L its electrical resistance) are unknown parameters.

Assumption 1: The unknown scalars a_p and b_p are such that $a_p < 0$ and $b_p > 0$.

We also assume that both the reference current $t \mapsto r(t)$ and its derivative $\dot{r}$ are available to the controller (see, e.g., [7, Rmk. 4] for a possible way of obtaining $\dot{r}$ by suitably filtering the reference r), and that they are both bounded, without necessarily knowing the bounds.

Assumption 2: The reference input $t \mapsto r(t)$ is a differentiable signal and both r and $\dot{r}$ are uniformly bounded.

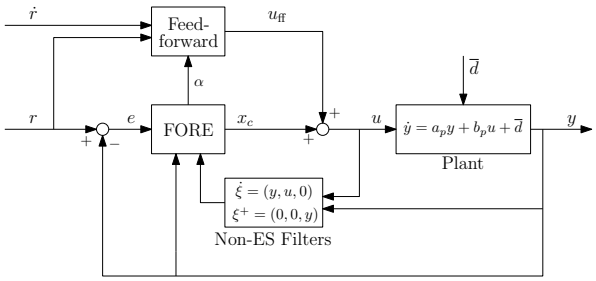

Fig. 1. Block diagram of the closed-loop architecture.

Our integrate-and-reset control scheme is sketched in Fig. 1. We discuss the feedforward action in Section III, while the feedback is performed by a First-Order Reset Element (FORE) [1], [15]. The FORE is a hybrid controller featuring an unstable continuous-time control action, which is appropriately reset to zero under specific conditions, to obtain stable hybrid trajectories [11]. Its dynamics is

$$\dot{x}_c = a_c x_c + b_c e, \qquad \dot{\tau}_{\rm r} = 1, \qquad (e, x_c, \tau_{\rm r}) \in \mathcal{F}_{\rm r}, \tag{2a}$$
$$x_c^+ = 0, \qquad \tau_{\rm r}^+ = 0, \qquad (e, x_c, \tau_{\rm r}) \in \mathcal{J}_{\rm r}, \tag{2b}$$

with the controller state being $x_c \in \mathbb{R}$ and the addition of a timer state $\tau_{\rm r}$ ("r" stands for "reset"), to ensure that the controller output is sufficiently regular. The scalars a_c, b_c are typically positive (generating an unstable continuous-time action) and they can be arbitrarily tuned, as we will show later in this Section. The jump and flow sets are defined as

$$\begin{aligned} \mathcal{F}_{\rm r} &:= \big\{(e, x_c, \tau_{\rm r}) : \varepsilon e^2 + 2 e x_c \geq 0 \text{ or } \tau_{\rm r} \leq \rho_{\min}\big\}, \\ \mathcal{J}_{\rm r} &:= \big\{(e, x_c, \tau_{\rm r}) : \varepsilon e^2 + 2 e x_c \leq 0 \text{ and } \tau_{\rm r} \geq \rho_{\min}\big\}, \end{aligned} \tag{2c}$$

where ε and $\rho_{\min}$ are small positive constants, as in [11]. Their choice has little effect on the closed-loop solutions if they are selected sufficiently small by "hierarchically" fixing ε small and then choosing $\rho_{\min}$ small enough [11]. The interconnection

$$u := x_c + u_{\rm ff}, \qquad e := r - y, \tag{3}$$

depicted in Fig. 1, gives the following continuous evolution for the tracking error (see [2, eq. (6)] for the derivations)

$$\dot{e} = a_p e - b_p x_c - d, \qquad e^+ = e, \tag{4}$$

where $d = b_p u_{\rm ff} - \dot{r} + a_p r + \bar{d}$ is a time-varying disturbance that should be canceled by the feedforward $u_{\rm ff}$. The complete hybrid dynamics of the feedback subsystem is

$$\begin{cases} \dot{x}_{\rm fb} = A_F x_{\rm fb} + B d, \\ \dot{\tau}_{\rm r} = 1, \end{cases} \quad x_{\rm fb}^\top M x_{\rm fb} \geq 0 \text{ or } \tau_{\rm r} \leq \rho_{\min}, \tag{5a}$$
$$\begin{cases} x_{\rm fb}^+ = A_J x_{\rm fb}, \\ \tau_{\rm r}^+ = 0, \end{cases} \quad x_{\rm fb}^\top M x_{\rm fb} \leq 0 \text{ and } \tau_{\rm r} \geq \rho_{\min}$$

where $x_{\rm fb} = (-e, x_c)$ and

$$\left[\begin{array}{c|c} A_F & B \\ \hline A_J & M \end{array}\right] = \left[\begin{array}{cc|cc} a_p & b_p & 1 & \\ -b_c & a_c & 0 & \\ \hline 1 & 0 & \varepsilon & -1 \\ 0 & 0 & -1 & 0 \end{array}\right]. \tag{5b}$$

The following proposition, whose proof is reported in [2, Prop. 1], provides useful degrees of freedom for the choice of the feedback controller parameters (a_c, b_c).

Proposition 1: Under Assumption 1, for any positive selection of the controller parameters $(a_c, b_c) \in \mathbb{R}_{>0} \times \mathbb{R}_{>0}$, the point $(e, x_c) = (0, 0)$ is globally exponentially stable (conditionally to hierarchically small ε and $\rho_{\min}$) for the reset feedback (2), and is finite gain exponentially input-to-state stable from the disturbance d to the state $x_{\rm fb}$.

III. Hybrid feedforward adaptation

If we knew the values $(a_p, b_p, \bar{d})$ of the plant parameters, we could select the feedforward term $u_{\rm ff}$ in Fig. 1 to be the ideal value $u_{\rm ff}^*$, corresponding to perfect cancellation of d in (4). With $\chi(r, \dot{r}) = [1 \;\; r \;\; \dot{r}]^\top$ known function of r and its derivative $\dot{r}$, and θ^* comprising the plant parameters

$$\theta^* := \begin{bmatrix} \theta_1^* & \theta_2^* & \theta_3^* \end{bmatrix}^\top = b_p^{-1} \begin{bmatrix} -\bar{d} & -a_p & 1 \end{bmatrix}^\top, \tag{6}$$

we may determine the ideal $u_{\rm ff}^*$ as

$$u_{\rm ff}^* = b_p^{-1}(\dot{r} - a_p r - \bar{d}) = \chi^\top(r, \dot{r})\theta^*. \tag{7}$$

Since θ^* in (6), (7) is unknown, we introduce a controller state θ representing its estimate, to be adapted via an integrate and reset mechanism. Then, based on (7), we select

$$u_{\rm ff} := \chi^\top(r, \dot{r})\theta \tag{8}$$

in such a way that $u_{\rm ff} \to u_{\rm ff}^*$ whenever $\theta \to \theta^*$.

Following previous reset-based sampled-data adaptations [5], [6], [13], we freeze the estimate θ during flows and we reset it at jumps, based on an integration phase (integrate and reset). More specifically, we augment the scheme with two integrators ξ_y, ξ_u and a memory element ξ_s, collected in the state $\xi = \big(\xi_y, \xi_u, \xi_s\big) \in \mathbb{R}^3$. We also use a timer $\tau_{\rm a}$ ("a" stands for "adaptation") and a symmetric matrix state $R \in \mathbb{R}^{3\times 3}$ (which may be called *information matrix*), which is kept constant during flows and is updated at jumps, just like θ. The feedforward dynamics is then

$$\begin{cases} \dot{\theta} = 0, \\ \dot{\xi} = \big(y, \; u, \; 0\big), \\ \dot{R} = 0, \end{cases} \quad \dot{\tau}_{\rm a} = 1, \qquad \tau_{\rm a} \in [0, \rho_{\max}], \tag{9a}$$
$$\begin{cases} \theta^+ = g_\theta(\theta, R, \xi, \tau_{\rm a}, y) \\ \xi^+ = \big(0, \; 0, \; y\big), \\ R^+ = g_R(R, \xi, \tau_{\rm a}, y), \end{cases} \quad \tau_{\rm a}^+ = 0, \qquad \tau_{\rm a} \in [\rho_{\min}, \rho_{\max}], \tag{9b}$$

where the update g_θ and g_R of θ and R are specified below. In (9), instead of exponentially stable filters (as in [5], [16]), we simply integrate, to avoid any forgetting effect before the update of θ. Once used in the update, the information in our integrators is reset to zero (integrate and reset).

The update of θ and R stems from the information on the evolution between two consecutive adaptations, collected in

$$\varphi := \begin{bmatrix} \tau_{\rm a} & \xi_y & y - \xi_s \end{bmatrix}^\top. \tag{10}$$

Inspired by the recursive least-squares (RLS) algorithm with directional forgetting [3], we use φ in (10) to define the update functions g_θ and g_R in (9b) as follows

$$g_\theta(\theta, R, \xi, \tau_{\rm a}, y) := \theta - P^+ \frac{\varphi}{\varphi^\top \varphi}\big(\varphi^\top \theta - \xi_u\big), \tag{11a}$$
$$g_R(R, \xi, \tau_{\rm a}, y) := R - \eta \Delta R + \Phi, \tag{11b}$$
$$\Delta R := \frac{R\varphi\varphi^\top R}{\varphi^\top R \varphi}, \quad \Phi := \frac{\varphi\varphi^\top}{\varphi^\top \varphi}, \tag{11c}$$

where $P := R^{-1}$ (which may be called *covariance matrix*) is always well defined due to Proposition 2 below. Matrix

Φ in (11c) is the projection matrix induced by the available direction φ, and the forgetting factor $\eta \in (0,1)$ multiplies the directions ΔR in (11c) to be partially forgotten. The equations in (11) are well defined at adaptations, since the first element of φ is $\tau_{\rm a}$, which is never zero, due to (9b).

The following proposition, which was stated as a conjecture in [2], shows that along solutions of (9)-(11) the information matrix R (or P^{-1}) evolves in the compact set

$$X_R := \left\{ R = R^\top \in \mathbb{R}^{3\times 3} : \alpha_m I \leq R \leq \eta^{-1} I \right\}, \quad (12)$$

for any $\alpha_m \in (0,1)$, in the sense that

$$R(0,0) \in X_R \implies R(t,j) \in X_R, \quad \forall (t,j) \in \operatorname{dom} R. \quad (13)$$

Note that in equation (13) solution $R(t,j)$ has a domain $\operatorname{dom} R$ comprising two times (continuous and discrete), as is typical for hybrid solutions [8]. We also emphasize that Proposition 2 is written for the case $X_R \in \mathbb{R}^{3\times 3}$ but applies to any other dimension. A related result is given in [3, Thm. 1-2], where only the existence of generic uniform lower and upper bounds for R are given. The statement of Proposition 2 is stronger, in that it explicitly characterizes set X_R as in (12), as a function of the parameters $\alpha_m < 1$ and $\eta < 1$.

Proposition 2: For any $\alpha_m \in (0,1)$ and $\eta \in (0,1)$, any solution to (9) with the update law (11b) satisfies (13).

Proof: Since g_R in (11b),(11c) does not depend on $|\varphi|$, without loss of generality, consider $|\varphi|^2 = \varphi^\top \varphi = 1$. Assuming $R \in X_R$, we prove below upper and lower bounds in (12) for $R^+ = R - \eta \Delta R + \Phi$ one by one.

Proof of $R^+ \geq \alpha_m I$: Given $R \in X_R$, each vector $v \in \mathbb{R}^3$ can be decomposed as $v = a\varphi + b\psi$, with $a, b \in \mathbb{R}$ and a suitable direction $\psi \in \mathbb{R}^3$ conjugate of φ with respect to R (dependent on v), which satisfies $\psi^\top R \varphi = 0$. By possibly scaling b, we select $|\psi|^2 = \psi^\top \psi = 1$. Then we have

$$\begin{aligned} v^\top R^+ v = a^2 \varphi^\top R \varphi + b^2 \psi^\top R \psi - \eta a^2 \varphi^\top R \varphi \\ + a^2 + 2ab\psi^\top \varphi + b^2 (\psi^\top \varphi)^2. \end{aligned}$$

Adding and subtracting $b^2 \alpha_m$ and rearranging, we obtain

$$\begin{aligned} v^\top R^+ v = \alpha_m (a^2 + b^2 + 2ab\psi^\top \varphi) \\ + (1-\alpha_m)(a^2 + 2ab\psi^\top \varphi) + b^2 (\psi^\top \varphi)^2 \\ + a^2 (1-\eta) \varphi^\top R \varphi + b^2 (\psi^\top R \psi - \alpha_m). \end{aligned}$$

Since $R \geq \alpha_m I$, the terms in the last line are non-negative, therefore

$$\begin{aligned} v^\top R^+ v &\geq \alpha_m (a^2 + b^2 + 2ab\psi^\top \varphi) + (1-\alpha_m) \\ &\quad \left(a^2 + 2ab\psi^\top \varphi + b^2 (\psi^\top \varphi)^2\right) + \alpha_m b^2 (\psi^\top \varphi)^2 \\ &= \alpha_m v^\top v + (1-\alpha_m)(a + b\psi^\top \varphi)^2 + \alpha_m b^2 (\psi^\top \varphi)^2 \\ &\geq \alpha_m |v|^2, \end{aligned}$$

which proves that $R^+ \geq \alpha_m I$, since v is any vector in $\mathbb{R}^3$.

Proof of $R^+ \leq \eta^{-1} I$: For each vector $v \in \mathbb{R}^3$, decompose it as $v = a\varphi + b\psi$, where $a, b \in \mathbb{R}$ and ψ is a conjugate direction of φ (dependent on v) satisfying $\psi^\top \varphi = 0$. Similar to the previous point, we can select $|\psi|^2 = \psi^\top \psi = 1$ by possibly rescaling b. We have

$$\begin{aligned} v^\top R^+ v &= a^2 \varphi^\top R \varphi + 2ab\psi^\top R \varphi + b^2 \psi^\top R \psi \\ &\quad - \eta a^2 \varphi^\top R \varphi - 2\eta ab \psi^\top R \varphi - \eta b^2 \frac{(\psi^\top R \varphi)^2}{\varphi^\top R \varphi} + a^2 \\ &= (1-\eta)(a\varphi + b\psi)^\top R (a\varphi + b\psi) + \eta b^2 \psi^\top R \psi \\ &\quad - \eta b^2 \frac{(\psi^\top R \varphi)^2}{\varphi^\top R \varphi} + a^2 \\ &= (1-\eta) v^\top R v + \eta b^2 \psi^\top R \psi - \eta b^2 \frac{(\psi^\top R \varphi)^2}{\varphi^\top R \varphi} + a^2. \end{aligned}$$

Using $R \leq \eta^{-1} I$, we obtain

$$v^\top R^+ v \leq \left(\eta^{-1} - 1\right) |v|^2 + \eta b^2 \psi^\top R \psi - \eta b^2 \frac{(\psi^\top R \varphi)^2}{\varphi^\top R \varphi} + a^2.$$

Since φ and ψ are orthogonal and with unit norm, we can substitute $a^2 - |v|^2 = a^2 |\varphi|^2 - |v|^2 = -b^2 |\psi|^2 = -b^2$ to get

$$\begin{aligned} v^\top R^+ v &\leq \eta^{-1} |v|^2 + b^2 \left(\eta \psi^\top R \psi - 1 - \eta \frac{(\psi^\top R \varphi)^2}{\varphi^\top R \varphi} \right) \\ &\leq \eta^{-1} |v|^2 + b^2 \left(\eta \psi^\top R \psi - 1 \right) \leq \eta^{-1} |v|^2, \end{aligned}$$

where the last inequality comes once again from the upper bound on R, and proves that $R^+ \leq \eta^{-1} I$, since v is any vector in $\mathbb{R}^3$, thus concluding the proof. ∎

IV. Stability analysis

Based on the nominal value of the parameter vector θ^* in (6), define the parameter estimation error

$$\tilde{\theta} := \theta - \theta^* \quad (14)$$

and the following scalar error variable

$$\begin{aligned} \tilde{\xi}_{\rm a}(t,j) := \frac{1}{b_p} \Bigg[\left(y(t_j, j) - \xi_s(t_j, j) \right) - a_p \Big(\xi_y - \int_{t_j}^{t} y(s,j) ds \Big) \\ - b_p \Big(\xi_u - \int_{t_j}^{t} u(s,j) ds \Big) - \bar{d} \Big(\tau_{\rm a} - (t - t_j) \Big) \Bigg], \end{aligned}$$

whose rationale is that, in view of (9), its evolution is

$$\begin{aligned} &\dot{\tilde{\xi}}_{\rm a} = 0, && \text{during flows,} \\ &\tilde{\xi}_{\rm a}^+ = \tilde{\xi}_{\rm a}, && \text{at feedback resets (2b),} \\ &\tilde{\xi}_{\rm a}^+ = 0, && \text{at feedforward resets (9b).} \end{aligned} \quad (15)$$

Additionally, introduce the transformed input $\chi_{\rm i}(t,j) := \int_{t_j}^{t} \chi(s,j) ds$, where t_j denotes the time of the last feedforward reset. Input $\chi_{\rm i}$ is uniformly bounded due to the boundedness assumed in Assumption 2. Introduce also the following error coordinate related to φ in (10)

$$\tilde{\varphi} := \varphi - \chi_{\rm i} := \varphi - \int_{t_j}^{t} \chi(s,j) ds, \quad (16)$$

which does not change across the feedback resets (2b) and is reset to zero across the feedforward resets (9b).

Using (5) and [2, Lemma 1-2], the error coordinates are

$$x := \left(x_{\rm fb},\ \tilde{\theta},\ \tilde{\varphi},\ \tilde{\xi}_{\rm a},\ R,\ \tau_{\rm r},\ \tau_{\rm a} \right) \in X, \quad (17)$$

where $X := \mathbb{R}^9 \times X_R \times [0, \rho_{\max}]^2$. The resulting error dynamics is obtained by defining $C := \left[\begin{smallmatrix} 0 & 0 \\ 1 & 0 \\ a_p & b_p \end{smallmatrix}\right]$, $F := \left[\begin{smallmatrix} 0 \\ 0 \\ 1 \end{smallmatrix}\right]$, using matrices Φ and ΔR in (11c), and using the selection

$$\Phi(\tilde{\varphi} + \chi_{\mathrm{i}}) := \frac{(\tilde{\varphi} + \chi_{\mathrm{i}})(\tilde{\varphi} + \chi_{\mathrm{i}})^\top}{(\tilde{\varphi} + \chi_{\mathrm{i}})^\top (\tilde{\varphi} + \chi_{\mathrm{i}})} = \frac{\varphi \varphi^\top}{\varphi^\top \varphi},$$

issued from (16), and similarly for $\Delta R(\tilde{\varphi} + \chi_{\mathrm{i}})$. From the relations in (5), (9)-(11), (15) and [2, Lemma 1-2], we get

$$\begin{cases} \dot{x}_{\mathrm{fb}} = A_F x_{\mathrm{fb}} + B b_p \chi^\top \tilde{\theta} \\ \dot{\tilde{\theta}} = 0 \\ \dot{\tilde{\varphi}} = C x_{\mathrm{fb}} + F b_p \chi^\top \tilde{\theta} \\ \dot{\tilde{\xi}}_a = 0, \quad \dot{R} = 0, \quad \dot{\tau}_{\mathrm{r}} = 1, \quad \dot{\tau}_{\mathrm{a}} = 1 \end{cases} \qquad x \in \mathcal{C}, \quad \text{(18a)}$$

$$\begin{cases} x_{\mathrm{fb}}^+ = x_{\mathrm{fb}} \\ \tilde{\theta}^+ = \big(I - P^+ \Phi(\tilde{\varphi} + \chi_{\mathrm{i}})\big)\tilde{\theta} - P^+ \dfrac{(\tilde{\varphi} + \chi_i)\tilde{\xi}_{\mathrm{a}}}{(\tilde{\varphi} + \chi_i)^\top (\tilde{\varphi} + \chi_i)} \\ \tilde{\varphi}^+ = 0, \quad \tilde{\xi}_{\mathrm{a}}^+ = 0 \\ R^+ = R - \eta \Delta R(\tilde{\varphi} + \chi_{\mathrm{i}}) + \Phi(\tilde{\varphi} + \chi_{\mathrm{i}}) \\ \tau_{\mathrm{r}}^+ = \tau_{\mathrm{r}}, \quad \tau_{\mathrm{a}}^+ = 0 \end{cases} \qquad x \in \mathcal{D}_{\mathrm{a}}, \quad \text{(18b)}$$

$$\begin{cases} x_{\mathrm{fb}}^+ = A_J x_{\mathrm{fb}} \\ \tilde{\theta}^+ = \tilde{\theta} \\ \tilde{\varphi}^+ = \tilde{\varphi}, \quad \tilde{\xi}_{\mathrm{a}}^+ = \tilde{\xi}_{\mathrm{a}} \\ R^+ = R \\ \tau_{\mathrm{r}}^+ = 0, \quad \tau_{\mathrm{a}}^+ = \tau_{\mathrm{a}} \end{cases} \qquad x \in \mathcal{D}_{\mathrm{r}}, \quad \text{(18c)}$$

with the jump and flow sets

$$\mathcal{C} := \{x \in X : x_{\mathrm{fb}}^\top M x_{\mathrm{fb}} \geq 0 \text{ or } \tau_{\mathrm{r}} \leq \rho_{\min}\}, \quad \text{(19a)}$$

$$\mathcal{D}_{\mathrm{a}} := \{x \in X : \tau_{\mathrm{a}} \geq \rho_{\min}\}, \quad \text{(19b)}$$

$$\mathcal{D}_{\mathrm{r}} := \{x \in X : x_{\mathrm{fb}}^\top M x_{\mathrm{fb}} \leq 0 \text{ and } \tau_{\mathrm{r}} \geq \rho_{\min}\}. \quad \text{(19c)}$$

The error dynamics (18) enjoys a useful pseudo-cascade structure, represented in Fig. 2. In particular, state $\tilde{\xi}_{\mathrm{a}}$ converges to zero in finite time as per (18) and drives a second subsystem with states $\tilde{\theta}, R, \tau_{\mathrm{a}}$, associated with the feedforward. Even though this subsystem is perturbed by the variable $\tilde{\varphi}$ (see Fig. 2), we show next that this perturbation provides zero gain in the stability bound. The third subsystem involves the feedback states $x_{\mathrm{fb}}, \tau_{\mathrm{r}}$ and is perturbed by $\tilde{\theta}$. Finally, the fourth subsystem, with state $\tilde{\varphi}$, is perturbed by the two previous ones. Perturbations also come from the external inputs χ, χ_{i}, which are bounded by assumption.

Remark 1: The hybrid system (18)-(19) satisfies the hybrid basic conditions [8, Ass. 6.5], therefore the system is well-posed, in view of [8, Thm. 6.8]. Well-posedness guarantees that stability is robust, ensuring that our control scheme can be used in practice, in the presence of small unmodeled phenomena and disturbances (see Section V). □

Our first main result is given below.

Theorem 1: The bounded and closed set (attractor)

$$\mathcal{A} := \big\{x \in X : \big(x_{\mathrm{fb}},\ \tilde{\theta},\ \tilde{\varphi},\ \tilde{\xi}_{\mathrm{a}}\big) = 0\big\} \quad \text{(20)}$$

is uniformly globally stable (UGS) for the error dynamics (18)-(19) for any positive selection of (a_c, b_c). Moreover, if $\tilde{\theta} \to 0$ then $x_{\mathrm{fb}} \to 0$.

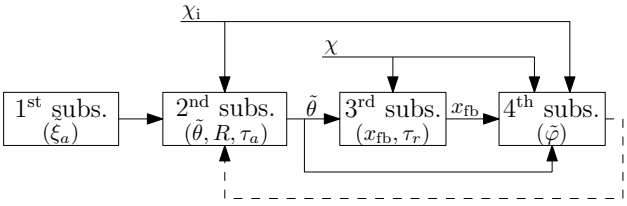

Fig. 2. Pseudo-cascade structure of the error dynamics (18).

Proof: Referring to Fig. 2, the state of the first subsystem $\tilde{\xi}_{\mathrm{a}}$ is always zero after the first jump from $\mathcal{D}_{\mathrm{a}}$, in view of (18). Thus, for simplicity we will consider $\tilde{\xi}_{\mathrm{a}} = 0$. Non-zero initial conditions for $\tilde{\xi}_{\mathrm{a}}$ could be taken into account by inflating the stability bound on $\tilde{\theta}$ by a finite amount. Indeed, $\tilde{\xi}_{\mathrm{a}}$ appears only in the expression of $\tilde{\theta}^+$ in (18b), with a uniformly bounded gain stemming from $|P^+| = |\,(R^+)^{-1}\,| \leq (\alpha_m)^{-1}$ (by Proposition 2) and from the fact that $|\tilde{\varphi} + \chi_i| = |\varphi| \geq \tau_{\mathrm{a}} > 0$ when $x \in \mathcal{D}_{\mathrm{a}}$, as mentioned after (11).

Second subsystem. To analyze the second subsystem with states $\tilde{\theta}$, R and τ_{a}, first note that these states are constant along flows due to (18a) and constant across feedback jumps (from $\mathcal{D}_{\mathrm{r}}$), due to (18c). Moreover, when $\tilde{\xi}_{\mathrm{a}} = 0$, the jumps of $R, \tilde{\theta}$ from $\mathcal{D}_{\mathrm{r}}$, described in (18b), correspond to the discrete-time RLS algorithm. Thus, consider the quadratic Lyapunov function $V(\theta, R) = \tilde{\theta}^\top R \tilde{\theta}$, and note that it satisfies

$$\alpha_m |\tilde{\theta}|^2 \leq V(\theta, R) \leq \eta^{-1} |\tilde{\theta}|^2, \quad \text{(21)}$$

due to the definition of the set X_R. Following the steps of the proof of [14, Thm. 3.1], we can then prove that V satisfies $V(\theta^+, R^+) - V(\theta, R) \leq 0$ across jumps from $\mathcal{D}_{\mathrm{a}}$.

Then, using (21), we can conclude that

$$\begin{aligned} |\tilde{\theta}(t,j)|^2 &\leq \alpha_m^{-1} \tilde{\theta}(t,j)^\top R(t,j) \tilde{\theta}(t,j) \quad \text{(22)} \\ &\leq \alpha_m^{-1} \tilde{\theta}(0,0)^\top R(0,0) \tilde{\theta}(0,0) \leq (\eta \alpha_m)^{-1} |\tilde{\theta}(0,0)|^2, \end{aligned}$$

which proves an UGS bound for the second subsystem, independent of the inputs $\tilde{\varphi}$ and χ_{i}, when $\tilde{\xi}_{\mathrm{a}} = 0$ (in a pseudo-cascade fashion).

Third subsystem. The UGS bound (22) for $\tilde{\theta}$ and the boundedness ensured by Assumption 2 imply that the input term $b_p \chi^\top \tilde{\theta}$ in (18a) (corresponding to d in (5)) at the right-hand side of $\dot{x}_{\mathrm{fb}}$ is bounded. This, together with the feedback loop being finite gain exponentially ISS from the input to x_{fb}, as proved in Proposition 1, allows proving the following exponential ISS bound for some suitable positive scalars $\kappa_3, \lambda_3, \gamma_3$

$$|x_{\mathrm{fb}}(t,j)| \leq \kappa_3 \mathrm{e}^{-\lambda_3 (t+j)} |x_{\mathrm{fb}}(0,0)| + \frac{\gamma_3}{\sqrt{\eta \alpha_m}} |\tilde{\theta}(0,0)|. \quad \text{(23)}$$

Fourth subsystem. The fourth subsystem simply provides an open-loop integral of bounded signals over a horizon length smaller than $\rho_{\max}$, therefore it satisfies, for some suitable positive scalars $\kappa_4, \lambda_4, \gamma_4$,

$$|\tilde{\varphi}(t,j)| \leq \kappa_4 \mathrm{e}^{-\lambda_4 (t+j)} |\tilde{\varphi}(0,0)| + \gamma_4 (\|x_{\mathrm{fb}}\|_\infty + \|\tilde{\theta}\|_\infty). \quad \text{(24)}$$

Pseudo-cascade argument. Combining the previous bounds we obtain and exponential ISS bound for the third and fourth

subsystems, uniform in χ and χ_{i}, which imply UGS of the overall interconnection, and convergence to zero of the states of the second and third subsystems, whenever $\tilde{\theta}$ (first subsystem) converges to zero, as to be proven.

Since the input term in $\dot{x}_{\text{fb}}$ linearly depends on $\tilde{\theta}$, finite gain exponential ISS from the input to x_{fb} also implies that $x_{\text{fb}} \to 0$ when $\tilde{\theta} \to 0$, thus concluding the proof. ■

Theorem 1 ensures that the estimation error and the tracking error do not diverge, for any positive choice of the controller gains and any external signals χ and χ_{i}. Convergence of x to the origin is ensured under a persistence of excitation requirement, similar to [14]. For simplicity of notation, we use $\{x\}$ to denote the sequence of values of the solution $x(t,j)$ before each feedforward jump (from $\mathcal{D}_{\text{a}}$).

Definition 1: The sequence $\{\Phi\}_h, h \in \mathbb{N}$ is *persistently exciting* (PE) if there exist $\varepsilon > 0, N > 0$ such that

$$\sum_{h=j}^{j+N-1} \frac{\{\Phi\}_h}{N} > \varepsilon I, \qquad \forall j \in \mathbb{N}. \tag{25}$$

Theorem 2: For any solution of the error dynamics (18), if the sequence $\{\Phi\}_h, h \in \mathbb{N}$ is PE, then $\lim_{t+j\to\infty} \theta(t,j) = \theta^*$, with exponentially fast convergence.

Proof: The proof is equivalent to the proof of [14, Thm. 3.2], noticing that the sequences $\{R\}_h, \{\theta\}_h$ are generated by a discrete-time RLS algorithm. ■

V. Experiments

A solenoid used in a pressure control valve was used for the experiments (see the photo in Fig. 5). Its nominal parameters are $\bar{R}_L$, $\bar{L}$. Moreover, all the current and voltage measurements are scaled to nominal values $\bar{i}$ and $\bar{V}$, respectively. The experiments were conducted on a *dSpace MicroLab Box* with sampling time $T_s = 1\,\text{ms}$ and PWM period $T_{\text{pwm}} = 50\,\mu\text{s}$. The current is sampled at a rate of $10\,\mu\text{s}$ and averaged over 100 measurements in order to mitigate the current ripple effects. The battery voltage v_{bat} supplies a calibrated power electronics circuit to generate the PWM voltages across the solenoid terminals.

Due to the choice of $\mathcal{D}_a$ in (19), our stability proofs allow for any sequence $\{\tau_{\text{a}}\}_h$ of feedforward reset intervals, as long as they all belong to $[\rho_{\text{min}}, \rho_{\text{max}}]$ (this includes periodic resets as a special case). Desirable choices of $\{\tau_{\text{a}}\}_h$ should be geared towards ensuring persistence of excitation. To this end, we suggest here to trigger feedforward resets when the condition numbers of R^+, R satisfy the inequality

$$\frac{\lambda_{\text{max}}(R^+)}{\lambda_{\text{min}}(R^+)} \leq K \text{e}^{\alpha\tau_{\text{a}}} \frac{\lambda_{\text{max}}(R)}{\lambda_{\text{min}}(R)}, \tag{26}$$

where α, K are positive scalar tunable parameters. Selection (26) is reasonable because $\alpha_m \leq \lambda_{\text{min}}(R)$ and $\eta^{-1} \geq \lambda_{\text{max}}(R)$, see (12). Therefore, the factor $(\eta\alpha_m)^{-1}$ in (22) is bounded from below by the condition number of R, i.e. $\lambda_{\text{max}}(R)/\lambda_{\text{min}}(R)$. Hence, according to (22), lowering the condition number of R favours a faster convergence of the parameters. Moreover, the increasing exponential at the right-hand side of (26) ensures a maximum dwell time. For the experiments we selected $K = 0.5$ and $\alpha = 10$ in (26).

The FORE parameters in (2) were chosen as $a_c = 11.9$, $b_c = 22.7$, $\varepsilon = 2 \cdot 10^{-3}$ and $\rho_{\text{min}} = 0.15$, leading to a desirable transient behavior. The forgetting factor in (11) was selected as $\eta = 0.15$, and the information matrix was initialized as $R(0,0) = \alpha_m I = 10^{-3} I$. The estimates were initialized at $R_L(0,0) = 0.9\bar{R}_L$, $L(0,0) = 5\bar{L}$, $\bar{d}(0,0) = 0$.

The experimental results are reported in Figs. 3-5. From Fig. 3 we can see that the estimates of R_L and L converge to their nominal values $\bar{R}_L$ and $\bar{L}$, respectively. For the (constant and unknown) disturbance d no nominal value $\bar{d}$ is available; however, we observe that its estimate converges to an equivalent input voltage $\bar{d}/\bar{L}$ two orders of magnitude

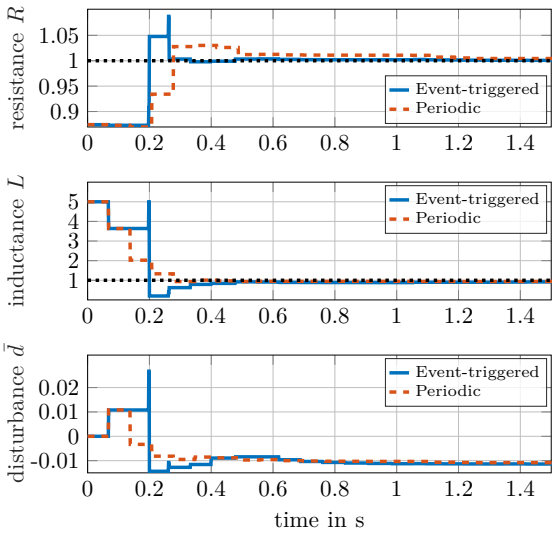

Fig. 3. Experimental time histories of the estimates of the three parameters using the feedforward reset trigger (26) (solid blue) and a periodic reset logic ($\rho_{\text{adapt}} = 70\,\text{ms}$, dashed orange): R_L (top), L (middle), $\bar{d}/\bar{L}$ (bottom). Values normalized to $\bar{R}_L$, $\bar{L}$ and $\bar{V}$, respectively.

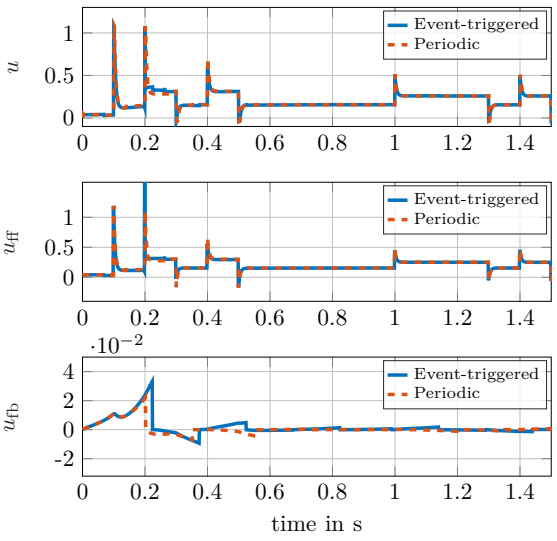

Fig. 4. Experimental plant inputs using the feedforward reset trigger (26) (solid blue) and a periodic reset logic, with $\rho_{\text{adapt}} = 70\,\text{ms}$ (dashed orange): measured voltage (top), computed feedforward input (middle), computed feedback input (bottom). Values normalized to $\bar{V}$.

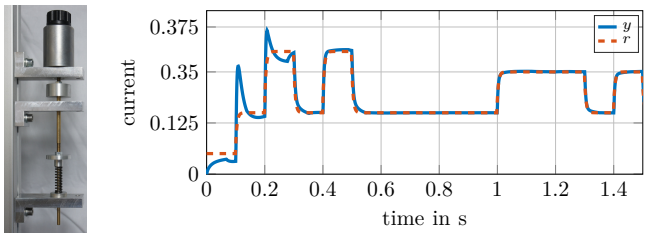

Fig. 5. Left: experimental solenoid. Right: output current (solid blue), and reference current (dashed orange). Values normalized to $\bar{i}$.

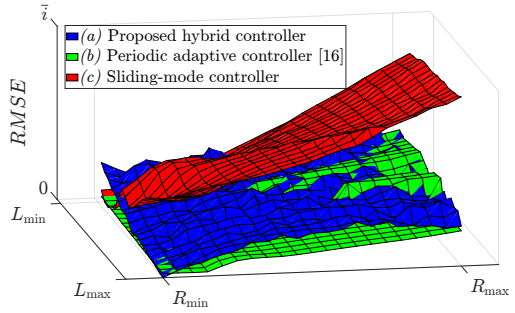

Fig. 6. Comparison of the performance of different control algorithms, in terms of root-mean square error, over a wide range of parameters. The value on the z-axis is normalized to $\bar{i}$.

smaller than the baseline voltage $\bar{V}$, which is reasonable.

Fig. 4 shows the voltage input, consisting in the feedforward u_{ff} and the feedback u_{fb} components, as commanded by the control algorithm. The bottom plot shows the typical trajectories of the feedback FORE, with exponentially diverging transients appropriately reset to zero [15]. After the initial transient, where the estimation and tracking error are driven to zero, the control input is mainly determined by the feedforward action. Moreover, even if the measured voltage does not exactly correspond to the commanded $u_{\text{ff}}+u_{\text{fb}}$ (due to actuation disturbances), we can see from Fig. 5 that the proposed controller correctly tracks the current reference, in view of the robustness properties discussed in Remark 1.

Finally, Fig. 6 compares different control algorithms in tracking the reference in Fig. 5. Specifically, we compare *(a)* our controller, *(b)* a 2-degreees-of-freedom adaptive controller [16], *(c)* a second-order sliding-mode controller [16, §V.A]. Controllers *(b)* and *(c)* are tuned as in [16].

We ran simulations over a wide range $R_{\min} \leq R_L \leq R_{\max}$ and $L_{\min} \leq L \leq L_{\max}$ of plant parameters (see the text after (1)), computing the root-mean square of the tracking error (RMSE) over 10s. Controller *(c)* is outperformed by the adaptive control schemes for the majority of the parameters combinations, while controllers *(a)* and *(b)* have comparable performance. Our hybrid scheme, however, achieves this result with fewer adaptations (the average interval between consecutive adaptations is 70ms, compared to 1ms for controller *(b)*) and with an event-triggered logic, thus enabling potential future improvements. These include determining triggering conditions that ensure the PE property, thus improving the algorithm robustness against parameter drift.

VI. Conclusions

We presented a feedback-feedforward control scheme for adaptive solenoid current tracking. The control algorithm features non-exponentially stable dynamics, both in the feedback, leading to aggressive control actions, and in the feedforward, preventing the loss of information before the parameter adaptations. We established stability results and illustrated their relevance in an experimental setup. Future work includes envisioning an event-triggered optimal choice of the adaptation instants inspired by the promising experimental results. The adaptation trigger can be connected to persistence of excitation properties on the parameters, to improve the robustness of the algorithm against parameter drift.

References

[1] A. Baños and A. Barreiro. *Reset control systems*. Springer, 2011.

[2] R. Bertollo, M. Schwegel, A. Kugi, and L. Zaccarian. Reset-control-based current tracking for a solenoid with unknown parameters. In *IFAC-ADHS*, volume 54, pages 199–204, 2021.

[3] L. Cao and H. Schwartz. A directional forgetting algorithm based on the decomposition of the information matrix. *Automatica*, 36(11):1725–1731, 2000.

[4] J. C. Clegg. A nonlinear integrator for servomechanisms. *Transactions of the American Institute of Electrical Engineers*, 77(1):41–42, 1958.

[5] M. Cocetti, S. Tarbouriech, L. Zaccarian, and M. Ragni. A hybrid adaptive inverse for uncertain SISO linear plants with full relative degree. In *ACC*, pages 2315–2320, 2019.

[6] M. Cordioli, M. Mueller, F. Panizzolo, F. Biral, and L. Zaccarian. An adaptive reset control scheme for valve current tracking in a power-split transmission system. In *ECC*, pages 1878–1883, 2015.

[7] F. Forni, S. Galeani, and L. Zaccarian. An almost anti-windup scheme for plants with magnitude, rate and curvature saturation. In *ACC*, pages 6769–6774, 2010.

[8] R. Goebel, R.G. Sanfelice, and A.R. Teel. *Hybrid Dynamical Systems: modeling, stability, and robustness*. Princeton University Press, 2012.

[9] I. Karafyllis, M. Kontorinaki, and M. Krstic. Adaptive control by regulation-triggered batch least squares. *IEEE Transactions on Automatic Control*, 65(7):2842–2855, 2020.

[10] C. Krimpmann, G. Schoppel, I. Glowatzky, and T. Bertram. Performance evaluation of nonlinear surfaces for sliding mode control of a hydraulic valve. In *IEEE Conf. on Control Applications*, pages 822–827, 2015.

[11] D. Nešić, A.R. Teel, and L. Zaccarian. Stability and performance of SISO control systems with first-order reset elements. *IEEE Transactions on Automatic Control*, 56(11):2567–2582, 2011.

[12] Y. Pan, T. Sun, and H. Yu. On parameter convergence in least squares identification and adaptive control. *International Journal of Robust and Nonlinear Control*, 29(10):2898–2911, 2019.

[13] F. S. Panni, H. Waschl, D. Alberer, and L. Zaccarian. Position regulation of an EGR valve using reset control with adaptive feedforward. *IEEE Transactions on Control Systems Technology*, 22(6):2424–2431, 2014.

[14] J. E. Parkum, N. K. Poulsen, and J. Holst. Recursive forgetting algorithms. *International Journal of Control*, 55(1):109–128, 1992.

[15] C. Prieur, I. Queinnec, S. Tarbouriech, and L. Zaccarian. Analysis and synthesis of reset control systems. *Foundations and Trends in Systems and Control*, 6(2-3):117–338, 2018.

[16] M. Schwegel, T. Glück, V. Shaferman, L. Zaccarian, and A. Kugi. Adaptive two-degrees-of-freedom current control for solenoids: Theoretical investigation and practical application. *IEEE Transactions on Control Systems Technology*, 31(3):1078–1091, 2023.

[17] X. Zhao, L. Li, J. Song, C. Li, and X. Gao. Linear control of switching valve in vehicle hydraulic control unit based on sensorless solenoid position estimation. *IEEE Transactions on Industrial Electronics*, 63(7):4073–4085, 2016.